Phys Chem Minerals (2017) 44:685–699
DOI 10.1007/s00269-017-0893-2

ORIGINAL PAPER

Roymillerite, $Pb_{24}Mg_9(Si_9AlO_{28})(SiO_4)(BO_3)(CO_3)_{10}(OH)_{14}O_4$, a new mineral: mineralogical characterization and crystal chemistry

Nikita V. Chukanov[1] · Erik Jonsson[2,3] · Sergey M. Aksenov[4,5,6] · Sergey N. Britvin[5] · Ramiza K. Rastsvetaeva[4] · Dmitriy I. Belakovskiy[7] · Konstantin V. Van[8]

Received: 21 February 2017 / Accepted: 21 April 2017 / Published online: 28 April 2017

Abstract The new mineral roymillerite $Pb_{24}Mg_9(Si_9AlO_{28})(SiO_4)(BO_3)(CO_3)_{10}(OH)_{14}O_4$, related to britvinite and molybdophyllite, was discovered in a Pb-rich assemblage from the Kombat Mine, Grootfontein district, Otjozondjupa region, Namibia, which includes also jacobsite, cerussite, hausmannite, sahlinite, rhodochrosite, barite, grootfonteinite, Mn–Fe oxides, and melanotekite. Roymillerite forms platy single-crystal grains up to 1.5 mm across and up to 0.3 mm thick. The new mineral is transparent, colorless to light pink, with a strong vitreous lustre. Cleavage is perfect on (001). Density calculated using the empirical formula is equal to 5.973 g/cm^3. Roymillerite is optically biaxial, negative, $\alpha = 1.86(1)$, $\beta \approx \gamma = 1.94(1)$, $2V$ (meas.) = 5(5)°. The IR spectrum shows the presence of britvinite-type tetrahedral sheets, CO_3^{2-}, BO_3^{3-}, and OH^- groups. The chemical composition is (wt%; electron microprobe, H_2O and CO_2 determined by gas chromatography, the content of B_2O_3 derived from structural data): MgO 4.93, MnO 1.24, FeO 0.95, PbO 75.38, B_2O_3 0.50, Al_2O_3 0.74, CO_2 5.83, SiO_2 7.90, H_2O 1.8, total 99.27. The empirical formula based on 83 O atoms *pfu* (i.e. $Z = 1$) is $Pb_{24.12}Mg_{8.74}Mn_{1.25}Fe_{0.94}B_{1.03}Al_{1.04}C_{9.46}Si_{9.39}H_{14.27}O_{83}$. The crystal structure was determined using single-crystal X-ray diffraction data. The new mineral is triclinic, space group $P\bar{1}$, with $a = 9.315(1)$, $b = 9.316(1)$, $c = 26.463(4)$ Å, $\alpha = 83.295(3)°$, $\beta = 83.308(3)°$, $\gamma = 60.023(2)°$, $V = 1971.2(6)$ Å^3. The crystal structure of roymillerite is based built by alternating pyrophyllite-type *TOT*-modules $Mg_9(OH)_8[(Si,Al)_{10}O_{28}]$ and *I*-blocks $Pb_{24}(OH)_6O_4(CO_3)_{10}(BO_3,SiO_4)$. The strongest lines of the powder X-ray diffraction pattern [*d*, Å (I, %) (*hkl*)] are: 25.9 (100) (001), 13.1 (11) (002), 3.480 (12) (017, 107, −115, 1–15), 3.378 (14) (126, 216), 3.282 (16) (−2–15, −1–25), 3.185 (12) (−116, 1–16), 2.684 (16) (031, 301, 030, 300, 332, −109, 0–19, 1–18), 2.382 (11) (0.0.–11). Roymillerite is named to honor Dr. Roy McG. Miller for his important contributions to the knowledge of the geology of Namibia.

Keywords New mineral · Roymillerite · Britvinite · Crystal structure · IR spectroscopy · Kombat Mine, Namibia

✉ Nikita V. Chukanov
chukanov@icp.ac.ru

[1] Institute of Problems of Chemical Physics, Russian Academy of Sciences, Chernogolovka, Moscow Region 142432, Russia

[2] Department of Mineral Resources, Geological Survey of Sweden, Box 670, 75128 Uppsala, Sweden

[3] Department of Earth Sciences, Uppsala University, 75236 Uppsala, Sweden

[4] Institute of Crystallography, Russian Academy of Sciences, 59 Leninskiy Prospekt, Moscow 117333, Russia

[5] Department of Crystallography, Saint Petersburg State University, Universitetskaya Nab. 7/9, St. Petersburg 199034, Russia

[6] Nesmeyanov Institute of Organoelement Compounds, Russian Academy of Sciences, GSP-1, Vavilova St. 28, V-334, Moscow 119991, Russia

[7] Fersman Mineralogical Museum of Russian Academy of Sciences, Leninskiy Prospekt 18-2, Moscow 119071, Russia

[8] Institute of Experimental Mineralogy, Russian Academy of Sciences, Chernogolovka, Moscow Region 142432, Russia

Introduction

Chalcophile elements, such as Pb, Sb, Bi, and Zn, are those metals and heavy semimetals which have a low affinity for

oxygen and a strong tendency to bond with sulfur and form sulfides and sulfosalts. Endogenic formations with chalcophile elements concentrated predominantly in oxygen-bearing minerals are relatively rare in nature. The most well-known occurrences of this type are Franklin and Sterling Hill Fe–Zn deposits in New Jersey, USA (Tarr 1929; Palache 1929a, b; Wilkerson 1962), Långban, Nordmark (including Jakobsberg) and Pajsberg (including Harstigen) Fe–Mn deposits in the Bergslagen ore province, Sweden (Palache 1929b; Moore 1970; Holtstam and Langhof 1999), metasomatic rocks of the "Mixed series" near Nežilovo in Macedonia (Chukanov et al. 2015), and parts of the Fe–Mn oxide ore units in the Kombat Mine in Namibia (Innes and Chaplin 1986; Dunn 1991). All of these localities are characterized by an extraordinarily wide variety of minerals, many of which are unknown from other localities. In particular, the Kombat Mine is the type locality of 13 mineral species (https://www.mindat.org/loc-2427.html).

The new mineral roymillerite, with the idealized formula $Pb_{24}Mg_9(Si_9AlO_{28})(SiO_4)(BO_3)(CO_3)_{10}(OH)_{14}O_4$, was discovered in the course of investigations of mineral associations from the Kombat Mine, situated in the Otavi Valley, 49 km south of Tsumeb, Grootfontein district, Otjozondjupa region, northern Namibia. The material carrying the new mineral was collected by miners during underground mining in the mid to the late 1980s or early 1990s. Based on comparisons with other samples collected at Kombat during this period, it seems likely that they originate from the locally Pb-(Cu)-rich, non-sulfide units situated within the Fe–Mn oxide ores of the Asis West Sector of the mine. Associated minerals in this case are jacobsite, cerussite, hausmannite, sahlinite, rhodochrosite, barite, grootfonteinite ($Pb_3O(CO_3)_2$, IMA 2015-051: Siidra et al. 2015), Fe–Mn oxides, and melanotekite.

The mineral is named to honor Dr. Roy McG. Miller (b. 1941) who has made important contributions to the knowledge of the geology of Namibia, beginning with his studies of Damara granites in the 1960s and progressing from there to include a wide range of rock types and geological formations. The mineral and its name have been approved by the IMA Commission on New Minerals, Nomenclature and Classification (IMA No. 2015-093). The holotype specimen is catalogued as # 20080176 at the Swedish Museum of Natural History, Stockholm, Sweden.

Properties of roymillerite

General appearance and physical properties

Roymillerite forms platy single-crystal grains and aggregates up to 1.5 mm across and 0.3 mm thick, occurring in a predominantly fine-grained groundmass of rhodochrosite, cerussite and other associated minerals (Fig. 1a, b). The only distinct form is {001}. The studied sample material exhibits a marked mineralogical and textural banding, potentially indicating an original layering; seemingly, roymillerite occurs mainly within a rhodochrosite band, while grootfonteinite occurs in a groundmass dominated by cerussite, with disseminated crystals and subhedral grains of Mn–(Fe) oxides, and locally euhedral to subhedral melanotekite. Granular aggregate of sahlinite platelets constitutes a separate band showing an indistinct foliation.

Roymillerite is transparent, colorless, and the streak is white. The lustre is strong, vitreous. Cleavage is perfect on (001); thin platelets are flexible, non-elastic. Fracture across cleavage is uneven. Parting has not been observed. The Mohs hardness is *ca.* 3. The density could not be measured because of the absence of heavy liquids with $D > 5$ g/cm^3. Density calculated using the empirical formula is equal to 5.973 g/cm^3.

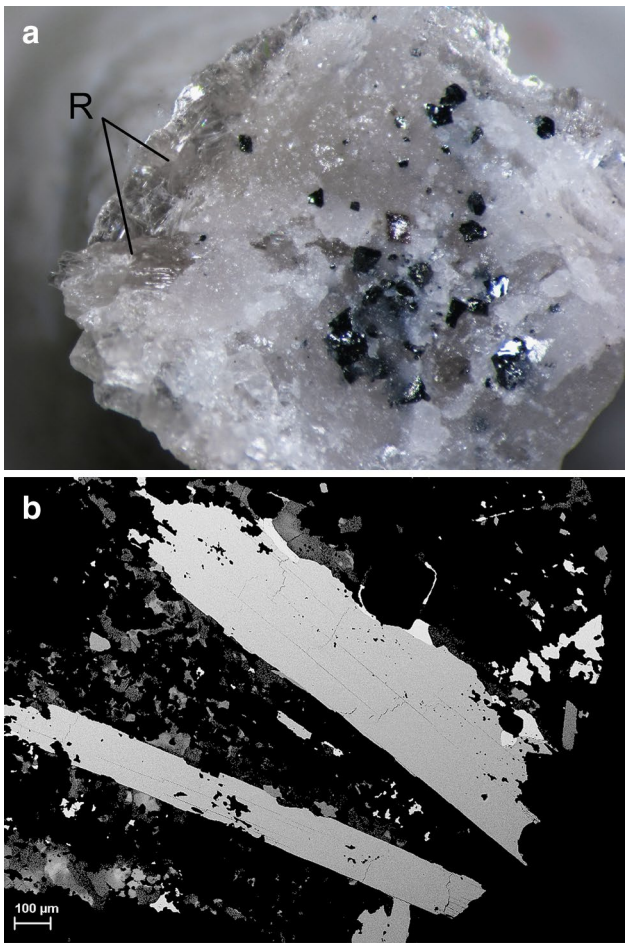

Fig. 1 **a** Aggregate of roymillerite platelets (*R*) intergrown with rhodochrosite and cerussite (*white*). *Black crystals* are jacobsite. Field of view 2.9 mm. **b** Platy crystals of roymillerite, showing distinct cleavage traces parallel to elongation, within a granular groundmass dominated by rhodochrosite. *Polished section* back-scattered electron (BSE) image

Optical properties

Roymillerite is nonpleochroic, colorless. It is optically biaxial, negative, $\alpha = 1.86(1)$, $\beta \approx \gamma = 1.94(1)$ ($\lambda = 589$ nm). $2V$ (meas.) = 5(5)°. Dispersion of optical axes was not observed. The orientation is: $X \approx c$.

The mineral is non-fluorescent under both long- and short-wave UV radiation.

Infrared absorption spectroscopy

To obtain infrared (IR) absorption spectra, powdered samples were mixed with anhydrous KBr, pelletized, and analyzed using an ALPHA FTIR spectrometer (Bruker Optics) with the resolution of 4 cm^{-1} in the wavenumber range from 360 to 3800 cm^{-1}; 16 scans were obtained. The IR spectrum of an analogous pellet of pure KBr was used as a reference.

Absorption bands in the IR spectrum of roymillerite (Fig. 2a) and their assignments are (cm^{-1}; s—strong band, w—weak band, sh—shoulder): 3700, 3583, 3513, 3352 (O–H stretching vibrations of OH^- groups), 2396w (possibly, acid Si–OH group), 1726w (combination mode), 1385 s (asymmetric stretching vibrations of CO_3^{2-} groups), 1231, 1204 (asymmetric stretching vibrations of BO_3^{3-} groups), 1083, 1050sh, 1042, 999 s (Si–O stretching vibrations of the Si_5O_{14} sheets), 915, 898, 875sh (Si–O stretching vibrations of isolated SiO_4^{4-} groups), 842w, 806w, 780w (out-of-plane vibrations of CO_3^{2-} groups, possibly combined with Mg···O–H and Pb···O–H bending vibrations), 725w, 688, 679 (in-plane vibrations of CO_3^{2-} groups, possibly combined with O–Si–O bending vibrations of the Si_5O_{14} sheets), 635w, 605w, 580w, 548w, 467 s, 420sh, 400sh (combination of Si–O–Si bending and Mg···O stretching vibrations).

The IR spectrum of roymillerite is similar to that of the related mineral britvinite (Chukanov et al. 2008; Fig. 2b). As compared with the latter, roymillerite is characterized by much stronger bands of CO_3^{2-} groups, their shifts, and the presence of an additional O–H-stretching band at 3513 cm^{-1}.

Chemical composition

Seven chemical analyses were carried out for Mg, Mn, Fe, Pb, Al, and Si using a digital scanning electron microscope Tescan VEGA-II XMU equipped with an Oxford INCA Wave 700 spectrometer (WDS mode, with an accelerating voltage of 20 kV, electron beam current of 20 nA, beam diameter of 3 μm, and a counting time of 100 s for each element). Calculations of the results of the X-ray microanalysis were carried out by means of the INCA Energy 300 software package. Contents of other elements with atomic numbers >8 are below their respective detection limits.

H_2O and CO_2 were determined by gas chromatography of products of ignition at 1200 °C. The content of B_2O_3 was derived from structural data. The presence of BO_3^{3-} groups is confirmed by the IR spectrum. Analytical data are given in Table 1.

The empirical formula of roymillerite (based on 83 O atoms per formula unit, i.e., $Z = 1$) is

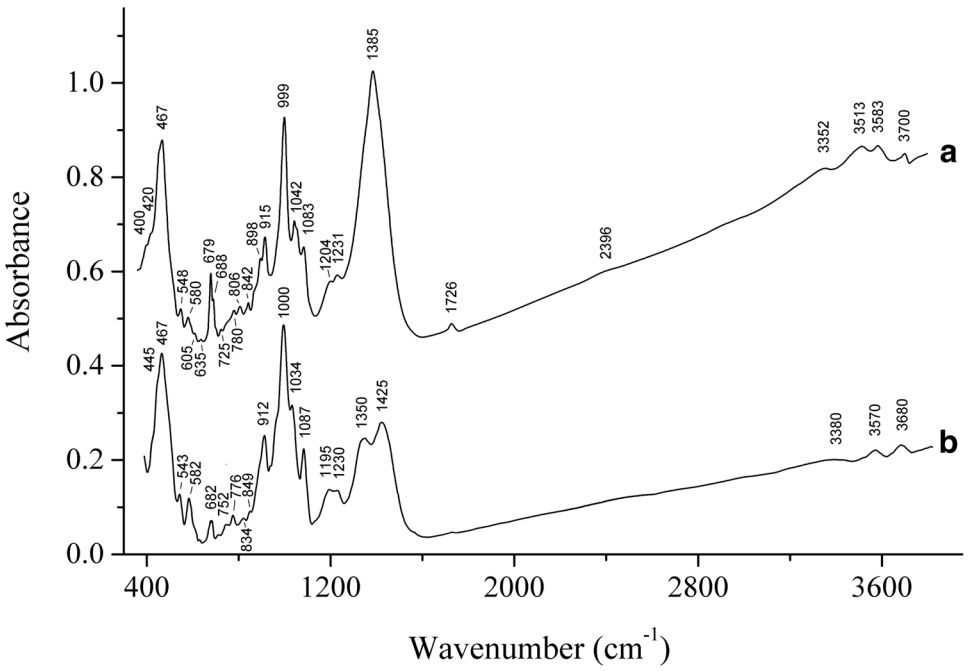

Fig. 2 Powder IR spectra of **a** roymillerite and **b** britvinite from Långban, Värmland, Sweden

Table 1 Chemical composition (in wt%) of roymillerite

Constituent	Mean	Range	Standard deviation	Probe standard
MgO	4.93	4.67–5.23	0.16	Diopside
MnO	1.24	1.03–1.45	0.12	$MnTiO_3$
FeO	0.95	0.81–1.03	0.08	Fe_2O_3
PbO	75.38	74.14–76.82	0.84	PbTe
B_2O_3	0.50			
Al_2O_3	0.74	0.64–0.88	0.08	Albite
CO_2	5.83 ± 0.15			
SiO_2	7.90	7.67–8.06	0.13	Albite
H_2O	1.8 ± 0.2			
Total	99.27			

$Pb_{24.12}Mg_{8.74}Mn_{1.25}Fe_{0.94}B_{1.03}Al_{1.04}C_{9.46}Si_{9.39}H_{14.27}O_{83}$. The simplified formula written in accordance with structural data (see below) is $Pb_{24}Mg_9(Si_9AlO_{28})(SiO_4)(BO_3)(CO_3)_{10}(OH)_{14}O_4$.

The Gladstone–Dale compatibility index (Mandarino 1981) calculated from the empirical formula and single-crystal unit-cell parameters is $1 - (K_P/K_C) = 0.000$ (superior).

X-ray diffraction data and crystal structure

Powder X-ray diffraction data for roymillerite were collected with a Rigaku R-AXIS Rapid II single-crystal diffractometer equipped with cylindrical image plate detector using Debye–Scherrer geometry (d = 127.4 mm), at an accelerating voltage of 40 kV and a current of 15 mA and 15 min exposure time. Data (in Å for Co$K\alpha$) are given in Table 2.

Unit-cell parameters of the triclinic unit cell refined from the powder data are: $a = 9.309(9)$ Å, $b = 9.331(9)$ Å, $c = 26.44(3)$ Å, $\alpha = 83.31(3)°$, $\beta = 83.30(3)°$, $\gamma = 59.87(4)°$, $V = 1968(2)$ Å^3.

Single-crystal X-ray diffraction patterns of roymillerite show low quality of crystals and are typically characterized by streaking (indicating staking disorder) and ill-defined reflections. Twinning was not observed. A colorless grain with the sizes 0.11 × 0.12 × 0.14 mm was used for single-crystal X-ray data collection. The data were collected at room temperature on a Bruker "Kappa Apex Duo" diffractometer with graphite-monochromatized Mo$K\alpha$ radiation (λ = 0.71073 Å) and a CCD detector using the $\omega - \theta$ scanning mode. Raw data were integrated and then scaled, merged, and corrected for Lorentz-polarization effects (APEX2 2009). A semiempirical absorption correction based upon the intensities of equivalent reflections was applied using SADABS (Sheldrick, 2008). A total of 29,590 reflections within the sphere limited by $\theta = 30.64°$ were measured. Based on R_{int} values, the primitive triclinic unit cell, space group $P\bar{1}$ (no. 2) was chosen with the following parameters: $a = 9.3152(15)$, $b = 9.3164(15)$, $c = 26.463(4)$ Å, $\alpha = 83.295(3)°$, $\beta = 83.308(3)°$, $\gamma = 60.023(2)°$; $V = 1971.2(6)$ Å^3. This cell can be transformed via the matrix [−1 −1 0/1 −1 0/0 0 1] to a pseudomonoclinic C-centered pseudocell with $a = 16.134$, $b = 9.319$, $c = 26.463$, $\beta = 97.74°$; $V = 3942.4$ Å^3, $R_{int} \sim 45\%$.

A structure model was determined by the "charge flipping" method, using the SUPERFLIP computer program (Palatinus and Chapuis 2007). The structure determination and refinement were carried out using the Jana2006 program package (Petříček et al. 2006). Illustrations were produced with the JANA2006 program package in combination with the program DIAMOND (Brandenburg and Putz 2005). Atomic scattering factors for neutral atoms together with anomalous dispersion corrections were taken from *International Tables for X-Ray Crystallography* (Ibers and Hamilton 1974). The experimental details of the data collection and refinement results are listed in Table 3.

The final refinement cycles converged with $R_1 = 5.71$, w$R_2 = 9.08$, GOF = 1.02 for 11,532 independent reflections with $I > 3\sigma(I)$. The highest positive peak and deepest minimum in the final residual electron-density map are 6.91 and −2.55 eÅ^{-3}, respectively. The rather large final values of $\Delta\rho_{min}$ and $\Delta\rho_{max}$ could be explained by the disordering of lead atoms. However, attempts to split sites failed because displacement parameters of additional sites became negative. Like in the structure of molybdophyllite (Kolitsch et al. 2012), the largest residual peaks were located at the levels of Pb layers which indicates the OD character of roymillerite structure.

Table 4 shows the fractional atomic coordinates, atomic displacement parameters and bond-valence sums. Selected interatomic distances are given in Table 5.

Discussion

Crystal structure

The crystal structure of roymillerite is related to those of molybdophyllite (Kolitsch et al. 2012) and britvinite (Yakubovich et al. 2008), and is based on a pyrophyllite-type *TOT*-module, which alternates with the lead-oxo-carbonate *I*-block (Fig. 3). As a result, the crystal-chemical formula of roymillerite can be written as follows ($Z = 1$): $^{I}\{Pb_{24}(OH)_6O_4(CO_3)_{10}[(BO_3)_{0.5}(SiO_4)_{0.5}]_2\}^{TOT}\{Mg_9(OH)_8[(Si,Al)_{10}O_{28}]\}$.

The *TOT*-module in the structure of roymillerite is similar to that in the structures of molybdophyllite and britvinite and contains a central *O* (octahedral) sheet of

Table 2 Powder X-ray diffraction data (d in Å) for roymillerite

d_{obs} (Å)	I_{obs} (%)	d_{calc} (Å)[a]	I_{calc} (%)[a]	*hkl*
25.9	100	26.2	100	001
13.1	11	13.1	13	002
8.73	2	8.74	2	003
8.01	3	8.05, 8.05, 7.99	1, 1, 2	010, 100, 110
7.89	2	7.85, 7.85	0.5, 0.5	011, 101
7.27	1	7.37	1	−1 to 11
7.05	3	7.08, 7.08	2, 2	012, 102
6.53	2	6.555	1	004
6.45	1	6.45	3	−1 to 12
6.15	1	6.13, 6.13	1, 1	013, 103
5.42	1	5.44	0.5	114
5.23	1	5.26, 5.26	0.5, 0.5	014, 104
4.92	3	4.92, 4.92	2, 2	−104, 0–14
4.68	1	4.68	1	115
4.63	2	4.65, 4.63, 4.63	0.5, 0.5, 2	211, 120, 210
4.58	3	4.59	3	1–11
4.53	4	4.53	5	122
4.46	4	4.47, 4.47	2, 4	−1 to 21, −2 to 11
4.38	5	4.39, 4.39	4, 3	−112, 1–12
4.297	5	4.301	7	213
4.207	4	4.211	7	− 1 to 22
4.106	2	4.112	4	−113
4.030	1	4.026, 4.025	0.2, 0.2	020, 200
4.005	2	4.006	1	214
3.926	2	3.939, 3.939	1, 1	0–21, −201
3.901	3	3.904	2	−2 to 13
3.824	2	3.835	2	223
3.792	4	3.797, 3.777, 3.777	3, 1, 1	1–14, −202, 0–22
3.744	2	3.755, 3.754	1, 1	023, 203
3.687	4	3.690, 3.687	5, 1	125, −2 to 22
3.628	2	3.634	4	–1–16
3.584	7	3.587	8	–2–14
3.480	12	3.488, 3.488, 3.484, 3.483	4, 4, 4, 10	017, 107, −115, 1–15
3.378	14	3.380, 3.380	9, 11	126, 216
3.317	5	3.331, 3.331, 3.304, 3.303	2, 2, 2, 2	−204, 0–24, 025, 205
3.282	16	3.284, 3.284	4, 16	−2 to 15, −1 to 25
3.225	1	3.225	2	−2 to 24
3.185	12	3.188, 3.187	15, 1	−116, 1–16
3.092	7	3.093	9	217
3.021	8	3.024, 3.024, 3.024, 3.024	4, 3, 4, 3	132, 230, 320, 312
2.981	4	2.987, 2.979	5, 1	−122, −1 to 31
2.964	4	2.962, 2.962, 2.962, 2.961	2, 1, 1, 2	−2–31, −3 to 21, 133, 313
2.916	6	2.919, 2.914	1, 1	1–17, 00–9
2.893	5	2.899, 2.891	4, 3	−1 to 18, −3 to 12
2.862	5	2.868, 2.867, 2.864,	2, 2, 2	−2 to 32, −3 to 22, 119
2.841	3	2.857, 2.856	2, 2	1–23, −213
2.793	4	2.801, 2.801, 2.793	3, 3, 1	019, 109, −124
2.784	4	2.779, 2.777	4, 4	−1 to 33, 325
2.756	2	2.758, 2.758, 2.752, 2.752	0.2, 0.2, 0.3, 0.3	−2 to 17, −1 to 27, −2 to 33, −3 to 23
2.739	2	2.738, 2.738	2, 1	−214, 1–24

Table 2 continued

d_{obs} (Å)	I_{obs} (%)	d_{calc} (Å)[a]	I_{calc} (%)[a]	*hkl*
2.684	16	2.688, 2.688, 2.684, 2.684, 2.682, 2.682, 2.682, 2.681	7, 7, 5, 5, 1, 1, 1	031, 301, 030, 300, 332, −109, 0–19, 1–18
2.653	3	2.652, 2.650	3, 3	−3 to 14, 236
2.620	7	2.622	4	0.0.–10
2.537	2	2.538	2	−2 to 18
2.519	1	2.517	1	−1 to 35
2.486	1	2.486, 2.485	0.2, 0.2	−3 to 25, 137
2.469	2	2.471, 2.470	0.3, 1	–216, 1–19
2.458	2	2.458, 2.458, 2.457	1, 1, 1	−3 to 33, 035, 305
2.425	2	2.436, 2.425	1, 1	0–34, 336
2.382	11	2.384	9	0.0.–11
2.345	1			
2.323	3			
2.302	2			
2.293	2			
2.281	2			
2.261	2			
2.251	2			
2.232	2			
2.214	3			
2.194	2			
2.173	3			
2.150	2			
2.123	4			
2.106	1			
2.080	2			
2.071	3			
2.056	1			
2.041	1			
2.024	4			
2.020	4			
2.002	3			
1.978	3			
1.961	2			
1.953	2			
1.940	1			
1.934	2			
1.928	2			
1.924	2			
1.910	2			
1.899	1			
1.872	2			
1.845	3			
1.829	1			
1.812	2			
1.789	1			
1.773	1			
1.760	3			
1.754	4			
1.751	4			
1.746	3			

Table 2 continued

d_{obs} (Å)	I_{obs} (%)	d_{calc} (Å)[a]	I_{calc} (%)[a]	*hkl*
1.741	3			
1.725	2			
1.708	1			
1.703	1			
1.689	1			
1.668	3			
1.658	1			
1.638	2			
1.615	1			
1.605	1			
1.593	2			
1.589	2			
1.587	2			
1.576	2			
1.562	3			
1.551	3			
1.546	3			
1.544	3			
1.525	1			
1.521	1			
1.517	2			
1.512	3			
1.490	2			
1.463	2			
1.445	1			
1.435	1			
1.429	1			
1.424	1			
1.418	1			
1.404	1			
1.399	1			
1.387	1			
1.379	1			
1.378	1			
1.371	1			
1.356	1			
1.345	1			
1.342	1			
1.337	1			
1.334	1			
1.327	1			
1.325	1			
1.324	1			
1.318	1			
1.311	1			
1.309	1			

Assignment of the reflections with *d* below 2.35 Å is ambiguous

[a] Calculated for unit-cell parameters obtained from single-crystal data

Table 3 Crystal parameters, data collection and structure refinement details for roymillerite

Crystal data	
Simplified formula	$Pb_{24}Mg_9(Si_9AlO_{28})(SiO_4)(BO_3)\ (CO_3)_{10}(OH)_{14}O_4$
Formula weight (g)	3479.5
Temperature (K)	293
Cell setting	Triclinic
Space group	$P\ \bar{1}$
a (Å)	9.3152(15)
b (Å)	9.3164(15)
c (Å)	26.463(4)
α (°)	83.295(3)
β (°)	83.308(3)
γ (°)	60.023(2)
V (Å^3)	1971.2(6)
Z	2
Calculated density, D_x (g cm^{-3})	5.973
Crystal size (mm)	0.11 × 0.12 × 0.15
Crystal form	Anhedral grain
Data collection	
Diffractometer	Bruker "Kappa Apex Duo"
Radiation; λ	MoK_α; 0.71073
Absorption coefficient, μ (mm^{-1})	51.406
F (000)	2959
Data range θ (°); h, k, l	0.78–30.64; $-13 < h < 13$, $-13 < k < 11$, $-37 < l < 37$
No. of measured reflections	29,590
No. total (N_2)/unique (N_1) reflections	11,532/9306
Criterion for observed reflections	$I > 3\sigma(I)$
R_{int}/R_σ (%)	4.86/5.56
Refinement	
Refinement on	Full-matrix least squares on F
Weight scheme	$1/(\sigma^2\|F\| + 0.0049F^2)$
R_1, wR_1	5.71, 8.05
R_2, wR_2	6.99, 9.08
GOF (goodness of fit)	1.02
Max./min. residual e density, (eÅ^{-3})	6.91/−2.55

$R_1 = \sum ||F_{obs}| - |F_{calc}|| / \sum |F_{obs}|$; $wR_2 = \{\sum [w(F^2_{obs} - F^2_{calc})^2] / \sum \{w(F^2_{obs})^2\}\}^{1/2}$
GOF $= \{\sum [w(F^2_{obs} - F^2_{calc})^2] / (n-p)\}^{1/2}$ where n is the number of reflections and p is the number of refined parameters

edge-sharing $MgØ_6$-octahedra (where Ø = O, OH) linked to two sheets of $(Si,Al)O_4$-tetrahedra (T-sheets). The tetrahedral (Si_5O_{14}) sheet is represented by a britvinite-type net with large 12-membered rings (Fig. 4).

The U_{iso} values for the Mg atoms are quite low which indicates partial substitution of Mg with Mn/Fe. However, the <Mg–O> distances (2.10–2.09 Å) do not indicate any preference of Mn/Fe for any of the Mg sites. In accordance with Kolitsch et al. (2012) and Yakubovich et al. (2008), small amounts of Al are assumed to substitute for Si.

The I-block in the structure of roymillerite contains ten "lead" layers and four "carbonate" layers, whereas in the structures of britvinite and molybdophyllite there are seven "lead" layers and two "carbonate" layers (Yakubovich et al. 2008), and four "lead" layers and one "carbonate" layer (Kolitsch et al. 2012), respectively.

The Pb atoms in the structure of roymillerite are ordered and occupy polyhedra with coordination numbers from five to seven, average distances Pb–O from 2.47 to 2.68 Å, and long weak bonds with Pb–O >3 Å (Table 5). Thus, these Pb^{2+} cations are characterized by the stereoactivity of their lone electron pairs.

Adjacent pairs of "lead" layers are separated by "carbonate" layer built by isolated CO_3-groups. Two

Table 4 Fractional coordinates, equivalent/isotropic displacement parameters of atoms (U, Å^2) and bond-valence sums (BVS, v.u.) in the structure of roymillerite

Site	x	y	z	$U_{eq/iso}$*	BVS
Pb1	0.8072(2)	0.6488(2)	0.04284(5)	0.0190(7)	2.02
Pb2	0.1496(2)	0.0153(1)	0.04253(5)	0.0189(7)	2.00
Pb3	0.7558(2)	0.0382(2)	0.31693(5)	0.0159(6)	1.94
Pb4	0.9968(2)	0.2561(2)	0.31673(5)	0.0158(6)	1.90
Pb5	0.5157(2)	0.3068(2)	0.04264(6)	0.0196(7)	2.01
Pb6	0.1102(2)	0.6111(2)	0.25482(5)	0.0220(7)	1.89
Pb7	0.5378(2)	0.4971(2)	0.31698(5)	0.0161(6)	1.92
Pb8	0.4460(2)	0.9452(2)	0.24570(6)	0.0277(8)	1.85
Pb9	0.8777(2)	0.8664(2)	0.14569(6)	0.0263(7)	1.81
Pb10	0.3665(2)	0.6587(2)	0.14576(6)	0.0256(7)	1.80
Pb11	0.1585(2)	0.3781(2)	0.14580(6)	0.0262(8)	1.85
Pb12	0.7878(2)	0.2891(3)	0.20346(7)	0.049(1)	1.78
Si1	0.409(1)	–0.089(1)	0.3978(3)	0.008(1)	3.94
Si2	0.094(1)	–0.100(1)	0.3942(3)	0.009(1)	3.95
Si3	0.394(1)	0.248(1)	0.3939(3)	0.009(1)	3.91
Si4	0.747(1)	0.595(1)	0.3945(3)	0.010(1)	3.90
Si5	0.076(1)	0.582(1)	0.3971(4)	0.011(1)	3.94
Mg1	0.8358(5)	–0.0002(5)	0.4978(2)	0.004(1)*	2.04
Mg2	0.8324(4)	0.3351(5)	0.4973(1)	0.003(1)*	2.03
Mg3	0.5008(4)	0.3337(5)	0.4980(1)	0.002(1)*	2.06
Mg4	0.1673(5)	0.3322(5)	0.5002(2)	0.005(1)*	2.07
Mg5	0.5	0	0.5	0.004(1)*	2.06
C1	0.155(1)	0.652(2)	0.0573(4)	0.007(2)*	3.70
C2	0.814(2)	0.319(2)	0.0686(6)	0.021(3)*	3.90
C3	0.448(2)	0.283(2)	0.2338(6)	0.019(3)*	3.84
C4	0.790(2)	0.615(2)	0.2368(6)	0.021(3)*	3.85
C5	0.117(2)	0.945(2)	0.2350(5)	0.013(2)*	3.85
Si6	0.481(1)	0.980(1)	0.0941(3)	0.022(2)*	1.81
B	0.489(2)	0.985(2)	0.0578(5)	0.012(2)*	1.80
O1	0.399(1)	–0.102(1)	0.4596(3)	0.006(1)*	1.99
O2	0.250(1)	0.808(1)	0.2366(4)	0.022(4)	2.04
O3	0.396(1)	0.232(1)	0.4562(3)	0.006(1)*	1.91
O4	0.150(1)	0.512(1)	0.0578(4)	0.018(4)	1.91
O5	0.728(1)	0.569(1)	0.4576(3)	0.007(2)*	1.89
O6	0.065(1)	0.565(1)	0.4606(3)	0.006(1)*	1.92
O7	0.070(1)	–0.104(1)	0.4566(3)	0.008(3)	1.88
O8	0.125(1)	0.724(1)	0.3753(4)	0.019(2)*	1.94
O9	0.762(1)	0.443(1)	0.3651(4)	0.020(4)	1.86
O10**	0.397(1)	0.567(1)	0.4598(3)	0.010(3)	1.03
O11**	0.728(1)	0.232(1)	0.4600(4)	0.013(3)	1.15
O12	0.773(1)	0.268(1)	0.2848(3)	0.010(2)*	2.22
O13	0.410(1)	0.082(1)	0.3737(4)	0.021(2)*	2.01
O14	0.648(2)	0.612(2)	0.2313(5)	0.035(5)	1.69
O15	0.808(2)	0.185(2)	0.0665(5)	0.027(5)	1.94
O16**	0.269(1)	0.103(1)	0.5397(3)	0.009(2)*	1.09
O17**	0.068(1)	0.227(1)	0.4605(3)	0.008(2)*	1.08
O18	–0.098(1)	0.625(1)	0.3762(4)	0.020(4)	2.06
O19	0.789(1)	0.749(1)	0.2365(4)	0.017(4)	2.13
O20	0.553(1)	0.264(1)	0.3646(4)	0.021(4)	1.82
O21	0.306(1)	0.287(1)	0.2373(4)	0.019(4)	1.92
O22	0.972(1)	0.946(2)	0.2363(5)	0.031(5)	1.90
O23	0.961(1)	0.309(1)	0.0656(4)	0.022(2)*	1.80
O24**	0.829(1)	0.651(1)	0.1263(4)	0.022(4)	1.13
O25	0.496(2)	0.847(2)	0.0567(5)	0.028(5)	1.80
O26	0.221(1)	0.403(1)	0.3753(4)	0.017(4)	1.95
O27	0.297(1)	0.650(1)	0.0569(4)	0.021(4)	1.93
O28	0.927(2)	0.472(2)	0.2351(5)	0.031(5)	2.03
O29	0.256(1)	–0.086(1)	0.3740(4)	0.018(4)	2.17
O30	0.684(1)	0.462(1)	0.0662(4)	0.021(2)*	1.94
O31	0.130(1)	0.629(1)	0.1697(3)	0.009(2)*	1.89
O32**	0.434(1)	0.329(2)	0.1271(4)	0.024(4)	1.11
O33	0.582(1)	–0.241(1)	0.3743(4)	0.016(3)	2.03
O34	0.588(2)	0.151(2)	0.2307(5)	0.032(3)*	1.96
O35	0.343(2)	0.123(1)	0.0588(5)	0.031(5)	1.71
O36	0.443(2)	0.427(1)	0.2364(4)	0.023(4)	1.92
O37**	0.152(2)	0.938(1)	0.1269(4)	0.020(4)	1.09
O38	0.625(2)	0.998(2)	0.0570(5)	0.029(3)*	1.70
O39	0.018(1)	0.793(1)	0.0576(4)	0.016(4)	2.00
O40	0.113(2)	0.087(2)	0.2296(5)	0.033(3)*	1.87
O41	0.941(1)	0.054(1)	0.3648(4)	0.020(4)	1.89
O42***	0.464(3)	0.964(4)	0.164(1)	0.036(6)*	0.98

U_{eq} is defined as one third of the trace of the orthogonalized U_{ij} tensor. Occupancy factor of Si6-, B- and O42-sites is 0.5. Bond-valence sum (BVS) calculations were performed using the bond-length parameters from Krivovichev and Brown (2001) (Pb^{2+}–O), Brese and O'Keeffe (1991) (Si^{4+}–O), and Brown and Altermatt (1985) (Mg^{2+}–O; C^{4+}–O; B^{3+}–O). BVSs were obtained by multiplying the calculated sums with the refined site-occupancy factors

** OH^- groups

*** Partially protonated O atom

central "carbonate" layers contain heteropolyhedral $[(SiO_4)_{0.5}(BO_3)_{0.5}]$ cluster (Fig. 3) formed by half-occupied $Si6O_4$-tetrahedra and BO_3-triangle (the Si6–B distance is 0.95 Å]. This cluster is similar to that in the structure of britvinite (Yakubovich et al. 2008). One bond of the half-occupied $Si6O_4$-tetrahedra is quite long (Si6–O42 = 1.83 Å) which could be explained by partial protonation of the O42 oxygen atom. The <B–O> distance of 1.30 Å is rather small, consequently a partial CO_3-for-BO_3 substitution seems possible.

The *I*-block contains oxygen atoms and hydroxyl groups with the environment formed only by Pb atoms, which could be described in the terms of anion-centered crystal chemistry (Krivovichev et al. 2013). The O12- and O31-atoms are tetrahedrally coordinated forming $[OPb_4]$-tetrahedra with the average distances

Table 5 Selected interatomic distances in the structure of roymillerite

Bond		Distance	Bond		Distance
Pb1	O24	2.24(1)	Pb12	O12	2.13(1)
	O30	2.51(2)		O34	2.74(2)
	O25	2.55(1)		O14	2.77(2)
	O23	2.77(1)		O40	2.77(1)
	O4	2.84(1)		O28	2.84(2)
	O38	2.86(1)		O22	2.85(1)
	O39	2.96(1)		O36	2.87(1)
<Pb1–O>		2.68	<Pb12–O>		2.71
	O4	3.10(1)*	Si1	O29	1.61(2)
	O35	3.21(1)*		O1	1.62(1)
Pb2	O37	2.27(1)		O33	1.64(1)
	O23	2.51(1)		O13	1.65(2)
	O35	2.55(2)	<Si1–O>		1.63
	O15	2.79(1)	Si2	O29	1.60(2)
	O25	2.84(1)		O41	1.63(1)
	O39	2.86(1)		O7	1.64(1)
	O27	2.96(1)		O8	1.65(2)
<Pb2–O>		2.68	<Si2–O>		1.63
	O39	3.12(1)*	Si3	O26	1.62(1)
	O38	3.15(1)*		O13	1.62(2)
Pb3	O12	2.29(1)		O3	1.64(1)
	O41	2.33(1)		O20	1.65(2)
	O20	2.38(1)	<Si3–O>		1.63
	O22	2.65(1)	Si4	O18	1.61(2)
	O34	2.72(1)		O33	1.63(1)
<Pb3–O>		2.47		O9	1.64(2)
	O13	3.24(1)*		O5	1.66(1)
Pb4	O12	2.29(1)	<Si4–O>		1.64
	O9	2.35(1)	Si5	O18	1.62(2)
	O41	2.39(1)		O8	1.62(2)
	O28	2.67(1)		O26	1.65(1)
	O40	2.75(1)		O6	1.67(1)
<Pb4–O>		2.49	<Si5–O>		1.64
	O29	3.22(1)*	Mg1	O16	2.06(1)
Pb5	O32	2.27(1)		O11	2.06(1)
	O15	2.50(1)		O17	2.07(1)
	O38	2.53(1)		O7	2.12(1)
	O30	2.76(2)		O7	2.13(1)
	O27	2.85(1)		O1	2.14(1)
	O35	2.85(2)	<Mg1–O>		2.10
	O4	2.96(1)	Mg2	O11	2.05(1)
<Pb5–O>		2.67		O17	2.07(1)
	O27	3.08(1)*		O5	2.09(1)
	O25	3.17(2)*		O10	2.10(1)
Pb6	O31	2.23(1)		O6	2.10(1)
	O19	2.69(1)		O7	2.16(1)
	O21	2.70(1)	<Mg2–O>		2.10
	O36	2.71(1)	Mg3	O11	2.03(1)
	O2	2.71(2)		O10	2.07(1)
	O22	2.73(1)		O10	2.10(1)
	O28	2.73(2)		O1	2.11(1)
<Pb6–O>		2.64		O5	2.12(1)
Pb7	O12	2.32(1)		O3	2.12(1)
	O20	2.33(1)	<Mg3–O>		2.09
	O9	2.38(1)	Mg4	O16	2.06(1)
	O36	2.66(1)		O6	2.08(1)
	O14	2.71(1)		O17	2.08(1)
<Pb7–O>		2.48		O6	2.08(1)
	O33	3.23(1)*		O5	2.11(1)
Pb8	O42	2.15(3)		O3	2.11(1)
	O2	2.74(2)	<Mg4–O>		2.09
	O14	2.76(1)	Mg5	O1	2.07(1) × 2
	O40	2.76(2)		O16	2.07(1) × 2
	O21	2.77(1)		O3	2.13(1) × 2
	O19	2.77(1)	<Mg5–O>		2.09
	O34	2.79(2)	C1	O39	1.29(1)
<Pb8–O>		2.68		O27	1.32(2)
Pb9	O31	2.37(1)		O4	1.33(2)
	O24	2.39(2)	<C1–O>		1.31
	O39	2.53(1)	C2	O30	1.28(2)
	O19	2.74(1)		O15	1.28(3)
	O37	2.92(2)		O23	1.32(2)
	O22	2.94(2)	<C2–O>		1.29
<Pb9–O>		2.65	C3	O34	1.27(2)
	O38	3.21(1)*		O21	1.29(2)
	O15	3.25(1)*		O36	1.34(3)
Pb10	O31	2.36(1)	<C3–O>		1.30
	O37	2.39(1)	C4	O19	1.24(3)
	O27	2.53(1)		O28	1.30(2)
	O2	2.75(1)		O14	1.36(3)
	O32	2.90(2)	<C4–O>		1.30
	O36	2.93(1)	C5	O2	1.26(1)
<Pb10–O>		2.64		O40	1.30(3)
	O25	3.23(2)*		O22	1.34(2)
	O30	3.25(1)*	<C5–O>		1.30
Pb11	O31	2.37(1)	Si6	O35	1.61(1)
	O32	2.38(1)		O25	1.62(2)
	O4	2.50(1)		O38	1.64(2)
	O21	2.76(1)		O42	1.83(3)
	O28	2.90(1)	<Si6–O>		1.68
	O24	2.91(1)		B	0.95(1)
<Pb11–O>		2.64	B	O25	1.26(2)
	O35	3.19(1)*		O38	1.32(2)
	O23	3.28(2)*		O35	1.33(1)
			<B–O>		1.30

* Not considered in the calculation of the average bond-length, but have been included in the calculation of the bond-valence sums

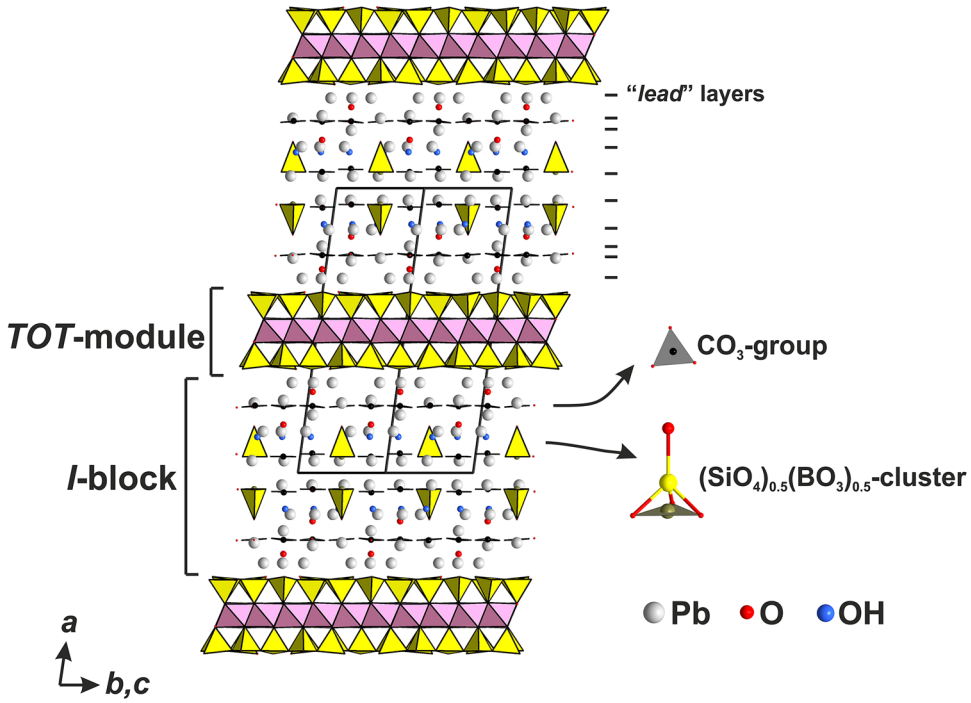

Fig. 3 General view of the crystal structure of roymillerite

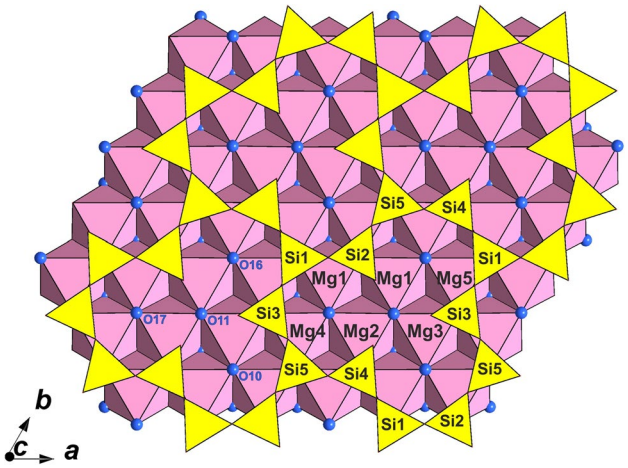

Fig. 4 *TOT*-module in the structure of roymillerite

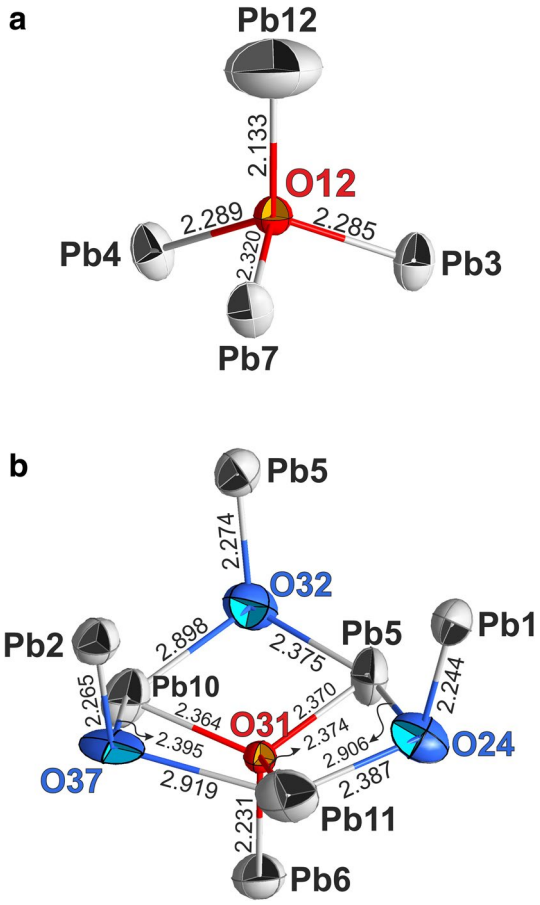

Fig. 5 Coordination environment of **a** the O12 atom and **b** cluster formed by anion-centered polyhedra

<O12–Pb> = 2.257 Å and <O31–Pb> = 2.335 Å, whereas O24, O32, and O37 sites of O atoms of OH groups are triangularly coordinated and form distorted anion-centered [$(OH)Pb_3$]-triangles (Fig. 5). The triangles are linked via common Pb–Pb edges with the [$O31Pb_4$]-tetrahedron forming a heteropolyhedral [$O(OH)_3Pb_7$]-cluster. Such a cluster was previously revealed in the structures of synthetic plumbonacrite $Pb_5O(OH)_2(CO_3)_3$ (Krivovichev and Burns 2000) and in a lead-exchanged variety of zeolite A (Kolitsch and Tillmanns 2003).

Table 6 Composition of the modules in the molybdophyllite–britvinite–roymillerite series

Mineral	*TOT*-module	*I*-block
Molybdophyllite[a]	$\{Mg_9[Si_{10}O_{28}(OH)_8]\}$	$2\cdot\{(OPb_4)(H_2O)_{0.5}(TO_3)_{1.5}\}$
Britvinite[a,b]	$\{Mg_9[Si_{10}O_{28}(OH)_8]\}$	$2\cdot\{[((O,F)Pb_4)Pb(TO_3)_3][(O,OH)_2Pb_2]\}$ or $2\cdot\{[(OPb_4)Pb(TO_3)_3][(O,OH)_2Pb_{2.5}]\}$
Roymillerite	$\{Mg_9[Si_{10}O_{28}(OH)_8]\}$	$2\cdot\{[(OPb_4)Pb(TO_3)_3][(O(OH)_3Pb_7)(TO_3)_3]\}$

[a] Kolitsch et al. (2012)

[b] Yakubovich et al. (2008)

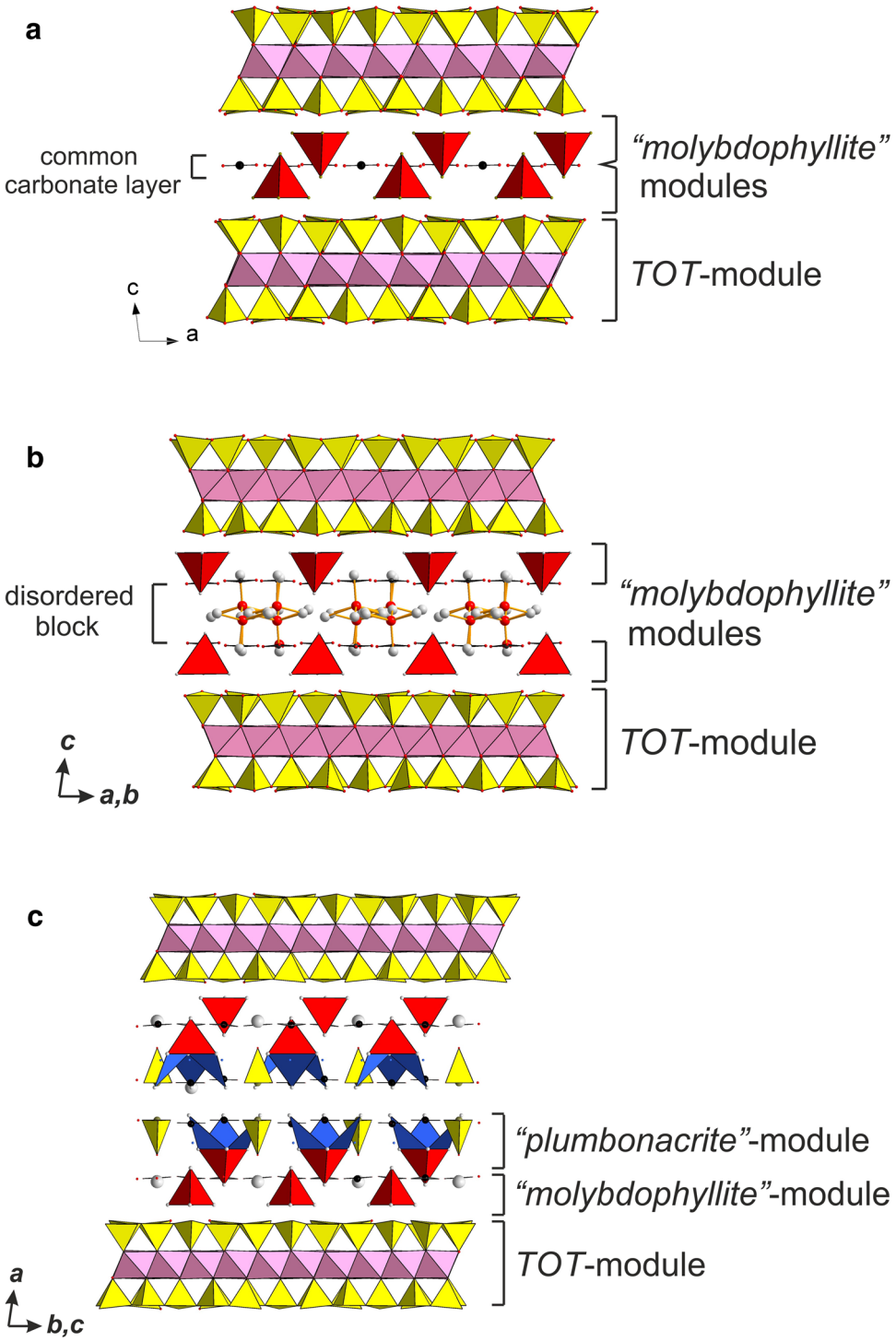

Fig. 6 Modular crystal structure of **a** molybdophyllite, **b** britvinite, and **c** roymillerite

Modularity of the molybdophyllite–britvinite–roymillerite series

The modular relationship between molybdophyllite and britvinite was described for the first time by Kolitsch et al. (2012). These authors showed that in terms of modular crystallography (Makovicky 1997), the two minerals belong to a common *merotypic* series and are characterized by the presence of a five-layer module with the composition $\{Mg_9[Si_{10}O_{28}(OH)_8](OPb_4)\}$. This module alternates with an *I*-block, having the composition $[(CO_3)_3{\cdot}H_2O]$ in molybdophyllite, and $\{[(OH)_3OPb_7][(BO_3)_3|(CO_3)_3]\}$ in britvinite.

Based on the data on the roymillerite structure, we have developed this approach and proposed a new view on modularity of the molybdophyllite–britvinite–roymillerite series. We consider only the three-layer *TOT*-module as a stable part of the structure. This is stable not only in the crystal-chemical meaning, but also taking into account chemical bonding. The whole intermodular part containing differently alternating simple lead-oxo-carbonate modules is considered as the *I*-block (Table 6).

In the structure of molybdophyllite, the *I*-block, with the composition $[(OPb_4)_2(H_2O)(CO_3)_3(BO_3)_3]$, can be divided into two "molybdophyllite" modules (Fig. 6). Each of them contains anion-centered (OPb_4)-tetrahedra and a "carbonate" layer which, being involved in the "molybdophyllite" module, is present also in the structures of britvinite and roymillerite (Fig. 6). The structure of molybdophyllite contains only one "carbonate" layer which is common for two adjacent "molybdophyllite" modules. Along with (OPb_4)-tetrahedra and (TO_3)-triangles, each module contain an additional *A*-site, which is occupied by a water molecule (in molybdophyllite) or Pb (in britvinite and roymillerite). Thus, the idealized formula of the "molybdophyllite" module could be written as follows: $\{(OPb_4)A(TO_3)_3\}$.

In the *I*-block of the britvinite structure (Yakubovich et al. 2008), "molybdophyllite" modules alternate with a quite disordered block of lead and oxygen atoms with the composition $\{(O,OH)_4Pb_4\}$ (Fig. 6). Kolitsch et al. (2012) refined the crystal structure of britvinite and reported the composition of the central block as $\{O(OH)_3Pb_5\}$ (excluding two Pb atoms of the *A* site). In the case of roymillerite, "molybdophyllite" modules alternate with "plumbonacrite" modules $[(O(OH)_3Pb_7)(TO_3)_3]$ which combine heteropolyhedral clusters and (TO_3)-groups (Fig. 7). At present, the molybdophyllite–britvinite–roymillerite series contains only three members, however, one can expect to find additional members belonging to this series, with different types of modules.

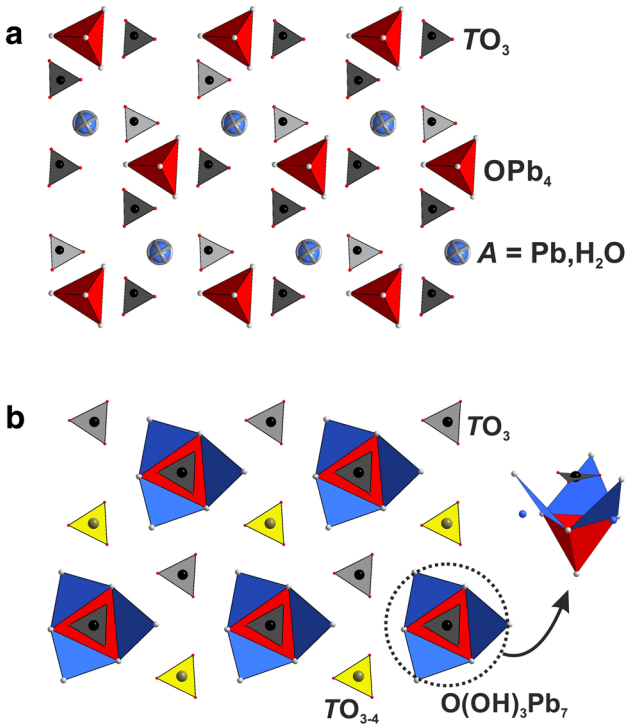

Fig. 7 General view of the **a** "molybdophyllite" and **b** "plumbonacrite" modules in roymillerite

Concluding remarks

As one can see from the above discussion, roymillerite, molybdophyllite and britvinite are related mineral species which have layered modular structures and form a *merotypic* series. The structures of these minerals are based on the *T*-layer $Si_{10}O_{28}$ (the britvinite-type net with large 12-membered rings) and the "molybdophyllite" module $(OPb_4)(H_2O,Pb)(CO_3)_3$. Molybdophyllite contains two adjacent "molybdophyllite" modules. In britvinite, "molybdophyllite" modules alternate with Pb-hydroxide blocks. In roymillerite, "molybdophyllite" modules alternate with "plumbonacrite" modules $[(O(OH)_3Pb_7)(TO_3)_3]$. Hypothetically, other representative of this *merotypic* series may exist with the similar building principles and various interleaves between "molybdophyllite" modules.

Comparative data for roymillerite, molybdophyllite and britvinite are given in Table 7. Despite roymillerite and britvinite are triclinic, and molybdophyllite is

Table 7 Comparative data for roymillerite and related minerals

Mineral	Roymillerite	Britvinite	Molybdophyllite
Formula	$Pb_{24}Mg_9(Si_9AlO_{28})(SiO_4)(BO_3)(CO_3)_1(OH)_{14}O_4$	$Pb_{15}Mg_9(Si_{10}O_{28})(CO_3)_2(BO_3)_4(OH)_{12}O_2$	$Pb_8Mg_9(Si_{10}O_{28})(CO_3)_3(OH)_8O_2{\cdot}H_2O$
Symmetry	Triclinic	Triclinic	Monoclinic
Space group	$P\bar{1}$	$P\bar{1}$	$C2$
a (Å)	9.1955	9.3409	16.232
b (Å)	9.2019	9.3597	9.373
c (Å)	26.1095	18.8333	14.060
α (°)	90.024	80.365	90
β (°)	96.720	75.816	97.36
γ (°)	119.912	59.870	90
V (Å^3)	1897.4	1378.74	2121.5
Z	1	1	2
Strong lines of the powder X-ray diffraction pattern: d (Å) (I, %)	25.9 (100)	18.1 (100)	14.23 (80)
	13.1(11)	3.39 (30)	3.073 (60)
	3.480 (12)	3.02 (90)	2.701 (70)
	3.378 (14)	2.698 (70)	2.684 (75)
	3.282 (16)	2.275 (30)	2.411 (70)
	3.185 (12)	1.867 (30)	1.772 (100)
	2.684 (16)	1.766 (40)	
	2.382 (11)	1.519 (40)	
Optical data			
α or ε	1.86	1.896	1.761
β or ω	1.94	1.896	1.815
γ	1.94	1.903	
2V, optical sign	−5°	−20°	(−) (<5–10)
Density, g/cm^3	5.973 (calculated)	5.42–5.51 (calculated)	4.652 (calculated) 4.72 (measured)
References	This work	Chukanov et al. (2008), Yakubovich et al. (2008)	Aminoff (1918), Welin (1968), Kolitsch et al. (2012), JCPDS 42-1384

monoclinic, the atomic arrangement in all these minerals is roughly pseudohexagonal.

Acknowledgements This work was financially supported by the Russian Foundation for Basic Research (Grant No. 16-35-60101-mol-a-dk) in part of structural investigations and Russian Science Foundation, Grant No. 14-17-00048 (in part of investigations of chemical composition and physical properties). The Department of Earth Sciences at the Swedish Museum of Natural History (Stockholm, Sweden), and specifically Jörgen Langhof, are thanked for the help with access to study and sample collection material. The authors are grateful to Uwe Kolitsch and Adam Pieczka for valuable comments.

References

Aminoff G (1918) Röntgenographische Ermittelung der Symmetrie und des Elementes p_0 des Molybdophyllits. Geol Fören Stockh Förh 40:923–938 **(in German)**

APEX2 (2009) Bruker AXS Inc., Madison, Wisconsin, USA

Brandenburg K, Putz H (2005) DIAMOND Version 3. Crystal Impact GbR, Bonn

Brese NE, O'Keeffe M (1991) Bond-valence parameters for solids. Acta Cryst B47:192–197

Brown ID, Altermatt D (1985) Bond-valence parameters obtained from a systematic analysis of the inorganic crystal structure database. Acta Cryst B 41:244–247

Chukanov NV, Yakubovich OV, Pekov IV, Belakovsky DI, Massa W (2008) Britvinite, $Pb_{15}Mg_9(Si_{10}O_{28})(BO_3)_4(CO_3)_2(OH)_{12}O_2$, a new mineral species from Långban, Sweden. Geol Ore Depos 50(8):713–719

Chukanov NV, Jančev S, Pekov IV (2015) The association of oxygen-bearing minerals of chalcophile elements in the orogenetic zone related to the "Mixed Series" complex near Nežilovo, Republic of Macedonia. Maced J Chem Chem Eng 34(1):115–124

Dunn PJ (1991) Rare minerals of the Kombat Mine. Mineral Record 22(6):421–425

Holtstam D, Langhof J (eds) (1999) Långban: the mines, their minerals, geology and explorers. Raster Förlag, Stockholm, p 217

Ibers JA, Hamilton WC (eds) (1974) International tables for X-ray crystallography, vol IV. The Kynoch Press, Birmingham

Innes J, Chaplin RC (1986) Ore bodies of the Kombat mine, South West Africa/Namibia. In: Anheusser CR, Maske S (eds) Mineral deposits of southern Africa. Geological Society of South Africa, Johannesburg, pp 1789–1805

Kolitsch U, Tillmanns E (2003) The crystal structure of anthropogenic Pb2(OH)3(NO3), and a review of Pb–(O, OH) clusters and lead nitrates. Mineral Mag 67:79–93

Kolitsch U, Merlino S, Holtstam D (2012) Molybdophyllite: crystal chemistry, crystal structure, OD character and modular relationships with britvinite. Mineral Mag 76:493–516

Krivovichev SV, Brown ID (2001) Are the compressive effects of encapsulation an artifact of the bond valence parameters? Z Kristallogr 216:245–247

Krivovichev SV, Burns PC (2000) Crystal chemistry of basic lead carbonates. II. Crystal structure of synthetic "plumbonacrite". Mineral Mag 64:1069–1075

Krivovichev SV, Mentré O, Siidra OI, Colmont M, Filatov SK (2013) Anion-centered tetrahedra in inorganic compounds. Chem Rev 113:6459–6535

Makovicky E (1997) Modularity—different types and approaches. In: Merlino S (ed) Modular Aspects of Minerals. Eötvös University Press, Budapest, pp 315–343

Mandarino JA (1981) The Gladstone–Dale relationship: part IV. The compatibility concept and its application. Can Miner 19:441–450

Moore PB (1970) Mineralogy and chemistry of Lingban-type deposits in Bergslagen, Sweden. Mineral Rec 1:154–172

Palache Ch (1929a) Paragenetic classification of the minerals of Franklin, New Jersey. Am Mineral 14(1):1–18

Palache Ch (1929b) A comparison of the ore deposits of Långban, Sweden, with those of Franklin, New Jersey. Am Mineral 14(2):43–47

Palatinus L, Chapuis G (2007) SUPERFLIP—a computer program for the solution of crystal structures by charge flipping in arbitrary dimensions. J Appl Crystallogr 40:786–790

Petříček V, Dušek M, Palatinus L (2006) Jana 2006. Structure determination software programs. Institute of Physics, Praha

Sheldrick GM (2008) A short history of SHELS. Acta Crystallogr A 64:112–116

Siidra OI, Jonsson E, Chukanov NV, Pekov IV, Zinyakhina DO, Polekhovsky YS, Yapaskurt VO (2015) Grootfonteinite, IMA 2015-051. CNMNC Newsletter No. 27, October 2015, page 1226. Mineral Mag 79:1229–1236

Tarr WA (1929) The origin of the zink deposits at Franklin and Sterling Hill, New Jersey. Am Mineral 14:207–221

Welin E (1968) X-ray powder data for minerals from Långban and the related mineral deposits of Central Sweden. Arkiv för Mineralogi och Geologi 4(30):499–541

Wilkerson AS (1962) The minerals of Franklin and Sterling Hill, New Jersey. Bulletin 65. New Jersey Geological Survey. Department of Conservation and Economic Development, Trenton

Yakubovich OV, Massa W, Chukanov NV (2008) Crystal structure of britvinite $[Pb_7(OH)_3F(BO_3)_2(CO_3)][Mg_{4.5}(OH)_3(Si_5O_{14})]$: a new layered silicate with an original type of silicon-oxygen networks. Crystallogr Rep 53(2):206–215